Outer region of the shock structure

The coordinates and the expansions are

$$x = \xi_0; \quad y = \epsilon Y_0(\xi_0) + \eta_0/Re$$

$$u = \cos\Phi + \delta^{3/4Pr}u_0 + \ldots; \quad v = -\sin\Phi + \delta^{3/4Pr}v_0 + \ldots \tag{2}$$

$$\rho = 1 + \delta^{3/4Pr}\rho_0 + \ldots; \quad p = p_0 + \ldots; \quad T = T_0 + \ldots$$

where ξ_0, η_0, u_0, ... are of order one. Since the maximum temperature in the flowfield is $O(T_0/\delta)$, cf. Eqs. (6, 10, and 13), the nondimensional emission rate Q is $O(\delta^{1-\omega})$ or smaller. Hence the radiation term of Eq. (1) can be written as

$$q_{\text{rad}} = -\delta^{-1}\Gamma\rho Q \leqq O(\Gamma\delta^{-\omega}) \tag{3}$$

For comparison, typical convection and conduction terms, respectively, are

$$q_{\text{conv}} = \rho v(\partial T/\partial y) = -Re \sin\Phi(\partial T_0/\partial\eta_0) + \ldots \tag{4}$$

$$q_{\text{cond}} = (\mu/PrRe)(\partial^2 T/\partial y^2) = RePr^{-1}T_0^{\omega}(\partial^2 T_0/\partial\eta_0^2) + \ldots$$

It follows that

$$(q_{\text{rad}}/q_{\text{conv}})_0 = O[(q_{\text{rad}}/q_{\text{cond}})_0] \leqq O(\Gamma/\delta^{\omega}Re) \rightarrow 0 \tag{5}$$

since $(\delta^{\omega}Re)^{-1} \leqq O(\epsilon) \rightarrow 0$ as has been shown by Bush.[3]

Middle region of the shock structure

$$x = \xi_m; \quad y = \epsilon Y_m(\xi) + \eta_m/\delta^{\omega}Re$$

$$u = u_m + \ldots; \quad v = v_m + \ldots; \quad \rho = \rho_m + \ldots \tag{6}$$

$$p = p_m/\delta + \ldots; \quad T = T_m/\delta + \ldots; \quad Q = Q_m + \ldots$$

Expanding the radiation term of Eq. (1) gives

$$q_{\text{rad}} = -\Gamma\delta^{-1}\rho Q = -\Gamma\delta^{-1}\rho_m Q_m + \ldots \tag{7}$$

Typical convection and conduction terms, respectively, are

$$q_{\text{conv}} = \rho v \frac{\partial T}{\partial y} = \delta^{\omega-1}Re\rho_m v_m \frac{\partial T_m}{\partial \eta_m} + \ldots$$

$$q_{\text{cond}} = \frac{\mu}{PrRe}\frac{\partial^2 T}{\partial y^2} = \delta^{\omega-1}RePr^{-1}T_m^{\omega}\frac{\partial^2 T_m}{\partial \eta_m^2} + \ldots \tag{8}$$

Hence

$$(q_{\text{rad}}/q_{\text{conv}})_m = O([q_{\text{rad}}/q_{\text{cond}}]_m) = O(\Gamma/\delta^{\omega}Re) \rightarrow 0 \tag{9}$$

Inner region of the shock structure

$$x = \xi_i; \quad y = \epsilon Y_i(\xi_i) + (\epsilon/\delta^{\omega}Re)\eta_i$$

$$u = W(\xi_i) + \epsilon u_i + \ldots; \quad v = \epsilon v_i + \ldots;$$

$$\rho = \rho_i/\epsilon + \ldots \tag{10}$$

$$p = p_i/\epsilon\delta + \ldots; \quad T = \delta^{-1}[\theta(\xi_i) + \epsilon T_i + \ldots];$$

$$Q = Q_i + \ldots$$

The radiation term of Eq. (1) becomes

$$q_{\text{rad}} = -\Gamma\epsilon^{-1}\delta^{-1}\rho_i Q_i \tag{11}$$

and, since $q_{\text{conv}}/q_{\text{cond}} = O(\epsilon) \rightarrow 0$ in this layer, q_{rad} has to be compared with the leading conduction terms, yielding

$$(q_{\text{rad}}/q_{\text{cond}})_i = O(\Gamma/\delta^{\omega}Re) \rightarrow 0 \tag{12}$$

Shock layer

$$x = \xi; \quad y = \epsilon\eta_L$$

$$u = u_L + \ldots; \quad v = \epsilon v_L + \ldots; \quad \rho = \rho_L/\epsilon + \ldots \tag{13}$$

$$p = p_L/\epsilon\delta + \ldots; \quad T = T_L/\delta + \ldots; \quad Q = Q_L + \ldots$$

The radiation term can be written as

$$q_{\text{rad}} = -\Gamma\epsilon^{-1}\delta^{-1}\rho_L Q_L + \ldots \tag{14}$$

Here the conduction terms are smaller or of the same order of magnitude as the leading convection terms. Thus, we compare the radiation term with a typical convection term to obtain

$$(q_{\text{rad}}/q_{\text{conv}})_L = O(\Gamma) = O(1) \tag{15}$$

The Eqs. (5, 9, 12, and 15) form the result that has already been discussed in the first section.

References

[1] Schneider, W., Comment on "Radiative Transfer in the Low Reynolds Number, Blunt-Body Stagnation Region at Hypersonic Speeds," *AIAA Journal*, Vol. 8, No. 6, June 1970, pp. 1180–1181.

[2] Liu, J. T. C., "Reply by Author to W. Schneider," *AIAA Journal*, Vol. 8, No. 6, June 1970, p. 1181.

[3] Bush, W. B., "On the Viscous Hypersonic Blunt Body Problem," *Journal of Fluid Mechanics*, Vol. 20, Part 3, Nov. 1964, pp. 353–367.

[4] Cheng, H. K., "Viscous Hypersonic Blunt-Body Problems and the Newtonian Theory," *Fundamental Phenomena in Hypersonic Flow*, edited by J. G. Hall, Cornell Univ. Press, Ithaca, N.Y., 1966, pp. 90–132.

[5] Schneider, W., "Effect of Radiation on Hypersonic Stagnation Flow at Low Density," *Zeitschrift fur Flugwissenschaften*, Vol. 18, No. 2/3, Feb./March 1970, pp. 50–58.

[6] Schneider, W., "Hypersonic Blunt-Body Flow of a Radiating Gas at Low Density," TR-32-1451, July 1970, Jet Propulsion Laboratory, California Institute of Technology, Pasadena, Calif.

[7] Liu, J. T. C. and Sogame, E., "Radiative Transfer in the Low Reynolds Number, Blunt-Body Stagnation Region at Hypersonic Speeds," *AIAA Journal*, Vol. 7, No. 7, July 1969, pp. 1273–1279.

[8] Penner, S. S. and Olfe, D. B., "Radiation and Reentry," Academic Press, New York, 1968, Chap. 3.

Flutter of a Buckled Plate Exposed to a Static Pressure Differential

C. S. Ventres*

Princeton University, Princeton, N.J.

Hess[1] has recently published an experimentally determined stability boundary for a panel exposed simultaneously to a static pressure differential and to a streamwise applied in-plane load. Prior efforts in this direction were either limited to panels free of applied in-plane loads,[2] or were carried out in a manner that did not provide precise control of the in-plane load, because of limitations inherent in the type of wind tunnel used.[3,4] In this Note, Hess' experimental results will be compared with a theoretical stability boundary calculated by the present author, using previously developed theoretical techniques.[5–7] The work represents an extension of previous work on flutter boundaries of pressure loaded plates free of externally applied in-plane loading.[5–7]

The panel tested by Hess had a length-width ratio of 2.88. The tunnel Mach number was 1.96. The panel flutter boundaries and flutter frequencies were determined at various values of static pressure differential and in-plane load. At each static pressure level, the in-plane load was varied until the minimum flutter dynamic pressure was realized. This minimum flutter dynamic pressure and the associated flutter fre-

Received October 15, 1970. The author would like to acknowledge helpful discussions with his colleague, E. H. Dowell. This work was supported by NASA Grant NGR 31-001-146.

* Member of the Research Staff.

quency are reproduced in Figs. 1 and 2. Note the pronounced increase in the minimum flutter dynamic pressure as the static pressure differential is raised (Fig. 1). In all cases the minimum flutter dynamic pressure was found to occur at an in-plane load close to the static buckling load for the appropriate Δp.[8]

The mathematical model and computational technique used to generate the theoretical results shown in Figs. 1 and 2 are discussed in detail in Ref. 7. Briefly, the structural theory is based on the von Kármán plate equations, while a quasi-steady (piston-theory) expression is used to represent the aerodynamic loading on the panel. This formulation is transformed into a set of modal equations of motion (nonlinear ordinary differental equations with the time τ as the independent variable) by Galerkin's method. Modal functions appropriate for a clamped plate were used. The modal equations are integrated numerically to determine the flutter amplitude w/h and flutter frequency K as a function of the dynamic pressure q, the stream-wise applied in-plane tension N_x, and the static pressure differential Δp. The flutter boundary is found by extrapolating to zero flutter amplitude. Each integration proceeds from an arbitrarily selected set of initial conditions. The flutter amplitude and frequency were not always independent of the initial conditions chosen, as will be discussed below.

Preliminary calculations indicated that the in-plane load at which the flutter dynamic pressure was minimized did not vary greatly with Δp. For simplicity, therefore, the curves in Figs. 1 and 2 were calculated for an in-plane load of 63 lb/in. (compression), which is roughly the buckling load for $\Delta p = 0$.

The flutter boundary for the case of zero in-plane edge restraint lies closest to the experimental results over the entire range of Δp (Fig. 1). This result is reminiscent of similar comparisons made previously for plates exposed to a static pressure differential alone (that is, with no applied in-plane load).[7] It can be seen that the largest percentage error occurs (for the assumption of zero edge restraint) near $\Delta p = 0$, where the panel is buckled, and is therefore sensitive to effects not included in the present analysis. Among these might be structural damping or initial panel imperfections. Either of these effects could have been included without difficulty, but the interpretation of the results would be open to question in view of the lack of any specific knowledge of these parameters. It was also found that for small static pressure differentials the transient time was much increased over that for large Δp and, correspondingly, the identification of the flutter motion was more difficult. In any case, interest here is centered on the results for $\Delta p \neq 0$, where the plate is stiffened by the static pressure differential, and these effects are no longer of great importance. In this region, the theoretical and experimental results agree rather well, although a more precise definition of the panel in-plane support conditions would be in order if a conservative but not unduly pessimistic flutter boundary were desired.

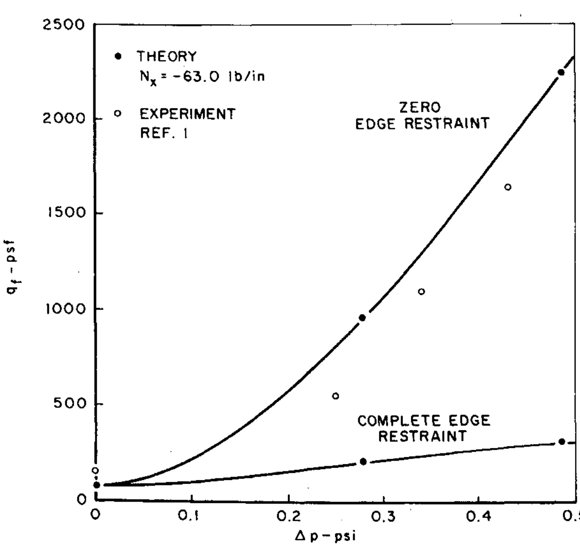

Fig. 1 Flutter dynamic pressure.

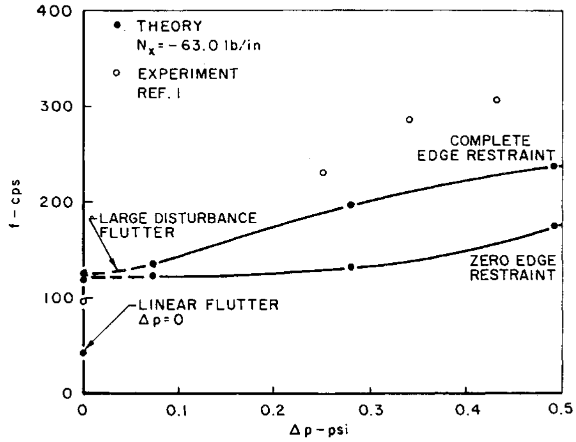

Fig. 2 Flutter frequency.

The theoretical flutter boundaries shown in Fig. 1 are the usual "small disturbance" or linear stability boundaries associated with the supposition of infinitesimal deviations from an equilibrium configuration of the panel. They were arrived at by using as initial conditions for the numerical integration a deflection configuration only slightly different from the static equilibrium configuration for the appropriate values of dynamic pressure, static pressure differential, and applied in-plane load. The flutter frequencies associated with these "linear" stability boundaries are shown as the solid lines in Fig. 2, as well as the dot labeled Linear Flutter at $\Delta p = 0$. The frequencies calculated were comparable to but not quantitatively close to the experimental results. This is perhaps not surprising, however, in view of the difficulty of representing exactly the elastic behavior of low aspect ratio plates with their closely spaced natural frequency spectra.

By choosing initial conditions for the integration that correspond to a panel shape significantly different from the equilibrium configuration, sustained panel oscillations were obtained for values of dynamic pressure less than the critical values shown in Fig. 1. The frequencies encountered differed substantially from the linear flutter frequencies only for small values of Δp. The dotted lines in Fig. 2 denote the fact that these "large disturbance" oscillations approach a frequency of about 120 cps as $\Delta p \rightarrow 0$, whereas the "linear" flutter frequency is only about 40 cps for $\Delta p = 0$. Such sustained oscillatory solutions have been computed once before in a regime stable with respect to sufficiently small "disturbances," for a buckled panel of length-width ratio 2.9.[7]

Presumably in an actual wind-tunnel test these "large disturbance" oscillations might be experienced in either of two ways: by providing (intentionally or otherwise) a disturbance of sufficient magnitude to excite the oscillations directly, or by operating the tunnel in such a way as to cross a (linear) flutter boundary from the unstable to the stable side. The panel would then exhibit a hysteresis pattern of behavior, in which panel oscillations would not be excited until the flutter boundary were reached if the boundary were approached from one side, but would be sustained well beyond the boundary if it were approached from the other. In the test procedure described by Hess,[1] all flutter boundaries were crossed from the stable to the unstable side, so that one might conjecture that no such oscillations were encountered. For this reason the linear "small disturbance" flutter boundaries displayed in Fig. 1 have been selected as being appropriate.

Conclusions

Using previously developed theoretical techniques, stability boundaries for a buckled plate exposed to a static pressure differential have been computed and compared to newly available experimental data. Flutter boundaries for plates with both zero and complete in-plane edge restraint were calculated. The effect of the static pressure differential is stabilizing for both extremes of in-plane restraint, but is very much more so for the case of zero restraint than for complete restraint. The experimental data lie closest to the stability boundary for zero restraint. All of these results are consistent with similar calculations and experimental correlations made previously for pressure loaded plates free of applied in-plane loads.

The calculated flutter frequencies are not in as good agreement with the experimental results as are the flutter boundaries. The theoretical results are complicated somewhat by the existence of sustained oscillatory solutions in flow regimes where normally the panel would be stable with respect to "small" disturbances. These solutions are interpreted as responses to large disturbances of the panel structure. Such large disturbance oscillations differ substantially from the linear flutter frequency only for very small static pressure differentials (where, for a buckled plate, the flutter motion is strongly amplitude dependent).

References

[1] Hess, R. W., "Experimental and Analytical Investigation of the Flutter of Flat Built-up Panels Under Streamwise In-Plane Load," TR-330, 1970, NASA.

[2] Dowell, E. H. and Voss, H. M., "Experimental and Theoretical Panel Flutter Studies in the Mach Number Range 1.0 to 5.0," ASD-TDR-63-449, June 1963, Aeronautical Systems Div., Wright-Patterson AFB, Ohio.

[3] Dixon, S. C. and Shore, C. P., "Effects of Differential Pressure, Thermal Stress and Buckling on Flutter of Flat Panels with Length-Width Ratio of 2," TN D-1949, 1963, NASA.

[4] Shideler, S. L., Dixon, S. C., and Shore, C. P., "Flutter at Mach 3 of Thermally Stressed Panels and Comparison with Theory for Panels with Edge Rotational Restraint," TN D-3498, 1966, NASA.

[5] Dowell, E. H., "Nonlinear Oscillations of a Fluttering Plate," *AIAA Journal*, Vol. 4, No. 7, July 1966, pp. 1267–1275.

[6] Dowell, E. H. and Ventres, C. S., "Nonlinear Flutter of Loaded Plates," AIAA Paper 68-286, Palm Springs, Calif., 1968.

[7] Ventres, C. S. and Dowell, E. H., "Comparison of Theory and Experiment for Nonlinear Flutter of Loaded Plates," *AIAA Journal*, Vol. 8, No. 11, Nov. 1970, pp. 2022–2030.

[8] Hess, R. W., Private communication, April 1970.

Supersonic Membrane Flutter

David J. Johns*

University of Technology, Loughborough, England

1. Introduction

Reference 1 has presented an interesting study of supersonic membrane flutter by considering the flutter of a two-dimensional plate in the presence of chordwise tensile in-plane stresses as the plate bending rigidity approaches zero. An asymptotic analysis using piston theory aerodynamics was developed based on the hypothesis of a boundary layer at the plate edge and several solutions were presented for analyses of various orders of approximation. These various solutions all showed that as the plate thickness approached zero, a simple flutter criterion was obtained viz.,

$$[2q/M\sigma_x][E^1/\sigma_x]^{1/2} = [\tfrac{2}{3}]^{3/2} \tag{1}$$

where $E^1 = E/12(1 - \nu^2)$ and the other symbols have their usual meaning.[1] The authors of Ref. 1 believed this to be a crude but conservative design criterion for the prevention of flutter of extremely thin two-dimensional plates at high Mach numbers.

Reference 2 has shown how the results of Ref. 1 may be generalized to include three-dimensional plates and other effects such as spanwise tensile in-plane stresses, structural damping, elastic foundation, orthotropicity, etc., based on the results of several other references, e.g., Ref. 3; and for Mach numbers from low subsonic through to high supersonic if the plate is of low aspect ratio.

The purpose of this Note is to show that the solution obtained in Ref. 1, as represented by Eq. (1), is a limiting result obtainable by the exact analysis of Ref. 4, which is a completely general study of supersonic flutter of flat rectangular orthotropic plates, and rather more general in its choice of boundary conditions than Ref. 3, which also contained exact analyses.

2. Analysis of Ref. 4

The governing differential equation for high supersonic speed flutter of a three-dimensional plate using two-dimensional static aerodynamics is given in Ref. 4 in terms of the chordwise deflection variable $X(x/a)$ as

$$X^{\mathrm{IV}}\left(\frac{x}{a}\right) + \pi^2\bar{A}X^{\mathrm{II}}\left(\frac{x}{a}\right) + \lambda X^{\mathrm{I}}\left(\frac{x}{a}\right) - \pi^4\bar{B}X\left(\frac{x}{a}\right) = 0 \tag{2}$$

where

$$\bar{A} = \left(\frac{a}{b}\right)^2\left[k_x + 2\left(\frac{D_{12}}{D_1}\right)\left(\frac{C_1}{\pi^2C_0}\right)\right] \tag{3}$$

$$\lambda = \frac{2qa^3}{\beta D_1}; \quad \beta = [M^2 - 1]^{1/2} \tag{4}$$

$$\bar{B} = \left(\frac{a}{b}\right)^4\left[\left(\frac{\omega}{\omega_0}\right)^2 - k_y\left(\frac{C_1}{\pi^2C_0}\right) - \left(\frac{D_2}{D_1}\right)\left(\frac{C_2}{\pi^4C_0}\right)\right] \tag{5}$$

and k_x, k_y are nondimensionalized in-plane compressive resultants for chordwise and spanwise loadings N_x,N_y respectively. C_0,C_1,C_2 are coefficients due to spanwise integrations of the spanwise modal deflection $Y(y/b)$ as indicated similarily in Ref. 2; D_1,D_2,D_{12} are appropriate rigidities of the orthotropic plate. Equation (5) can be generalized further to include the effect of an elastic foundation stiffness K as in Ref. 3, but this does not directly affect the critical flutter speed parameter λ_{cr} as will now be discussed.

The general solution to Eq. (2) with due consideration of the boundary conditions at $x = 0, a$, has been found in Ref. 4, and for large negative values of the parameter $\bar{A}$ (corresponding to large tensile chordwise in-plane stresses) a simple algebraic solution for λ_{cr} in terms of $\bar{A}$ is obtained as given below, which is applicable to simply supported or clamped boundary conditions on the spanwise edges $x = 0,a$;

$$\lambda_{cr} = [4\pi^3/3][10 - \bar{A}][(4 - \bar{A})/6]^{1/2} \tag{6}$$

The corresponding value of $\bar{B}_{cr}$, as given in Ref. 4 in terms of $\bar{A}$, defines the flutter frequency and it is seen therefore that the terms in k_y and K do not directly influence λ_{cr}.

Expanding the various terms in Eq. (6) for an isotropic plate one obtains

$$\lambda_{cr} = \frac{2qa^3}{\beta D} = \frac{4\pi^3}{3[6]^{1/2}}\left[10 - \frac{N_xa^2}{\pi^2D} + 2\,\frac{a^2}{b^2}\,\frac{C_1}{\pi^2C_0}\right] \times \left[4 - \frac{N_xa^2}{\pi^2D} + 2\,\frac{a^2}{b^2}\,\frac{C_1}{\pi^2C_0}\right]^{1/2} \tag{7}$$

Received September 18, 1970; revision received January 12, 1971.

* Professor.